

1
2
3
4 **Myofilament Glycation in Diabetes Reduces Contractility by Inhibiting**
5 **Tropomyosin Movement, is Rescued by cMyBPC Domains**
6
7

8 Maria Papadaki¹, Theerachat Kampaengsri¹, Samantha K. Barrick²,
9 Stuart G. Campbell³, Dirk von Lewinski⁴, Peter P. Rainer⁴, Samantha P. Harris⁵,
10 Michael J. Greenberg², Jonathan A. Kirk^{1†}

11
12 ¹ Department of Cell and Molecular Physiology, Loyola University of Chicago,
13 Maywood, Illinois, USA

14
15 ² Department of Biochemistry and Molecular Biophysics, Washington University in St
16 Louis, St Louis, Missouri, USA

17
18 ³ Department of Bioengineering, Yale University, New Haven, Connecticut, USA

19
20 ⁴ Division of Cardiology, Medical University of Graz, Graz, Austria

21
22 ⁵ Department of Cellular and Molecular Medicine, The University of Arizona, Tucson,
23 Arizona, USA

24
25
26
27
28 † Corresponding Author
29 Jonathan A. Kirk, Ph.D.
30 Department of Cell and Molecular Physiology
31 Loyola University Chicago Stritch School of Medicine
32 Center for Translational Research, Room 522
33 2160 S. First Ave.
34 Maywood, IL 60153
35 Ph: 708-216-6348
36 Email: jkirk2@luc.edu

37
38
39
40
41
42 Total Word Count: 7706
43 Figures: 7

44
45
46

47

Abstract

48 Diabetes doubles the risk of developing heart failure (HF). As the prevalence
49 of diabetes grows, so will HF unless the mechanisms connecting these diseases can
50 be identified. Methylglyoxal (MG) is a glycolysis by-product that forms irreversible
51 modifications on lysine and arginine, called glycation. We previously found that
52 myofilament MG glycation causes sarcomere contractile dysfunction and is
53 increased in patients with diabetes and HF. The aim of this study was to discover the
54 molecular mechanisms by which MG glycation of myofilament proteins cause
55 sarcomere dysfunction and to identify therapeutic avenues to compensate. In
56 humans with type 2 diabetes without HF, we found increased glycation of sarcomeric
57 actin compared to non-diabetics and it correlated with decreased calcium sensitivity.
58 Depressed calcium sensitivity is pathogenic for HF, therefore myofilament glycation
59 represents a promising therapeutic target to inhibit the development of HF in
60 diabetics. To identify possible therapeutic targets, we further defined the molecular
61 actions of myofilament glycation. Skinned myocytes exposed to 100 μ M MG
62 exhibited decreased calcium sensitivity, maximal calcium-activated force, and
63 crossbridge kinetics. Replicating MG's functional affects using a computer simulation
64 of sarcomere function predicted simultaneous decreases in tropomyosin's blocked-
65 to-closed rate transition and crossbridge duty cycle were consistent with all
66 experimental findings. Stopped-flow experiments and ATPase activity confirmed MG
67 decreased the blocked-to-closed transition rate. Currently, no therapeutics target
68 tropomyosin, so as proof-of-principle, we used a n-terminal peptide of myosin-
69 binding protein C, previously shown to alter tropomyosin's position on actin. C0C2
70 completely rescued MG-induced calcium desensitization, suggesting a possible
71 treatment for diabetic HF.

72

73 Word Count: 249/250

74

75

76 Keywords: Myofilament glycation, diabetes, myBPC C0C2, tropomyosin

77

78

Abbreviations

79

80 AG: Aminoguanidine

81 AGE: Advanced Glycation Endproducts

82 cMyBPC: cardiac myosin binding protein C

83 f : myosin binding rate

84 F_{\max} : maximal calcium-activated force

85 g_{xb} : myosin detachment rate

86 HF: Heart Failure

87 k : ATP detachment rate constant

88 K_B : blocked-to-closed rate transition

89 k_{tr} : rate of force redevelopment

90 LV: Left Ventricle

91 MG: Methylglyoxal

92 OM: Omecamtiv Mecarbil

93

94

95

96

Introduction

97 Almost half a billion people worldwide have type 2 diabetes mellitus (T2DM), a figure
98 that is expected to increase by ~40% within 25 years [1]. Diabetes doubles the risk
99 of developing heart failure [2, 3], independent of the effect on microvascular disease
100 and hypertension. Left unchecked, the rapid expansion of diabetes will result in an
101 explosion of heart failure cases. Therefore, it is critical that we discover the
102 underlying molecular mechanisms that link these two conditions so they might be
103 targeted therapeutically. We previously reported that one such link is likely mediated
104 by methylglyoxal (MG) [4], a reactive carbonyl species that is formed from the
105 degradation of triose phosphates [5] during glycolysis. MG can rapidly and
106 irreversibly react with arginine and lysine amino acids on proteins [6], a process
107 called glycation. Glycated proteins are known as advanced glycation end-products
108 (AGE), and can bind to Receptors of AGE on the cell surface [7], inducing a
109 signalling cascade resulting in oxidative damage and inflammation [8]. However, it is
110 also possible for glycation of these residues to act as post-translational modifications
111 that directly alter protein function, which is the mechanism explored in this study.

112 In recent years we and others have provided evidence that methylglyoxal may
113 play a role in the development of heart failure [7, 9] through glycation of intracellular
114 proteins involved in excitation-contraction coupling. For example, methylglyoxal can
115 react with Ryanodine Receptor and SERCA in the hearts of type I diabetic rats and
116 alter intracellular calcium handling [10, 11]. Our previous work, however, was the first
117 to make the connection in humans, showing that MG modifications were increased in
118 the cardiac myofilament of patients who had diabetes and heart failure, but not in
119 heart failure patients without diabetes or healthy patients [4]. These MG
120 modifications, occurring primarily on actin and myosin, reduced cardiomyocyte
121 myofilament calcium sensitivity and maximal calcium-activated force [4]. However,
122 whether MG modifications precede the development of overt systolic dysfunction,
123 and thus represent a possible cause of increased heart failure risk in diabetic
124 patients, is unknown. Genetic mutations in sarcomere proteins that reduce calcium
125 sensitivity are a cause of cardiomyopathy and heart failure [12]. Thus, if myofilament
126 glycation is elevated by diabetes and similarly reduce calcium sensitivity, they are
127 likely pathogenic for the development of heart failure.

128 Since methylglyoxal modifications are irreversible, there are two possible
129 approaches to correct the dysfunction: 1) decrease MG levels so these harmful

130 adducts are not formed in the first place, or 2) identify treatments that can
131 compensate for the dysfunction despite the continued presence of the MG
132 modifications. Genetic approaches to depress MG levels in animal models may be
133 beneficial, for example a recent study showing that AAV overexpression of Glo1, the
134 enzyme that catalyzes MG, in endothelial cells improves function in a rat model of
135 type 1 diabetes [13]. Unfortunately, approaches to reduce MG levels clinically have
136 already failed. Specifically, compounds called “AGE-breakers”, drugs aimed at
137 reducing levels of MG and AGE [14, 15] showed no benefit in clinical trials. In fact,
138 one trial in patients with type 2 diabetes was terminated early due to a negative
139 impact [16]. Our therapeutic strategy aims at correcting the dysfunction occurring at
140 the myofilament level, since the myofilament is a highly tuneable system [17] that is
141 likely amenable to this approach.

142 In this study, we show in diabetic human hearts without heart failure that MG
143 modifications are already increased compared to non-diabetics and correlate with
144 early myofilament dysfunction. A successful strategy for restoring function would
145 need to be informed by first discovering the molecular mechanism(s) by which MG
146 inhibited myofilament function. Therefore, we measured the impact of MG on
147 myofilament kinetics, used a computer model of myofilament activation to predict
148 molecular changes, and validated the predictions through biophysical assays. These
149 comprehensive approaches revealed that MG decreases the rate constant for the
150 transition of tropomyosin from its blocked state to its closed state on actin, effectively
151 making it harder to activate the thin filament. The n-terminal domain of cardiac
152 myosin binding protein C (cMyBPC) has been shown to activate the thin filament by
153 altering tropomyosin’s position on actin [18]. Indeed, the effects of MG on
154 myofilament calcium sensitivity were rescued by recombinant cMyBPC domains,
155 suggesting that targeting thin filament activation could be a viable therapeutic
156 strategy to break the connection between diabetes and heart failure.

157

158

Methods

159

160 Expanded Methods are presented in Supplemental Material

161

162 **Human and animal studies**

163 Human left ventricular tissue samples were obtained at the Medical University of
164 Graz from organ donors whose hearts were rejected for transplantation but did not
165 have heart failure. Human study protocols were approved by the Ethics Committee
166 at the Medical University of Graz (28-508 ex 15/16). All patients gave informed
167 consent and the investigation conformed to the principles outlined in the declaration
168 of Helsinki. Animal studies were approved by the Loyola University Chicago
169 Institutional Animal Care and Use Committee (IACUC number 2019029) according to
170 the NIH Guide for the Care and Use of Laboratory Animals. C57/Bl6J male mice 2-4
171 months of age were purchased from Jackson laboratories (Jackson labs, USA).
172 Animals were euthanised by placing them in an induction chamber with isoflurane
173 vaporizer (5%). The animal remained in the chamber until unconscious, as
174 determined by corneal reflex. Following isoflurane exposure, animals were
175 euthanised by cervical dislocation and heart extubating.

176

177 **Mass spectrometry**

178 Myofilament samples were prepared as stated previously [4]. Samples were
179 run on a 4-12% SDS- PAGE gel, stained with Coomassie stain, actin and myosin
180 bands excised, and then de-stained overnight. Gel bands were prepared for mass
181 spectrometry by digesting them in 2 µg/band Trypsin/LysC protease mix (Thermo
182 Scientific) for 16 hours at 37 °C. 200 - 300 ng of peptides were loaded onto an
183 UltiMate 3000 nanoHPLC coupled to a LTQ Orbitrap XL (Thermo). MS data analysis
184 was performed using the Peaks Bioinformatics Software. For analysis, glycated
185 peptides were normalized to the corresponding total peptides for each sample.

186

187 **Functional assessments and recombinant proteins**

188 Skinned myocytes were prepared as previously described [4, 19]. ATPase
189 activity and tension cost were measured in skinned fibers using an in-house system,
190 as previously [20, 21]. Cardiac myosin S1 and actin and tropomyosin were
191 expressed and purified as described in the Supplemental methods. Tropomyosin

192 blocked-to-closed state transition (KB) and ADP release were measured using
193 stopped-flow methods [22] (see Supplementary methods for details).

194

195 **Computational modelling**

196 A previously published model of myofilament Ca^{2+} activation [24] was used to
197 identify molecular changes to sarcomeric proteins that could plausibly explain
198 observed effects of methylglyoxal on skinned cardiac fibres. Baseline parameters
199 from the published model were used as a starting parameter set. The model was
200 implemented and run in MATLAB (Mathworks) as previously described.

201

202 **Statistical analysis**

203 Data are presented as mean \pm standard error. Quantitative data were
204 analysed using Prism 8 (GraphPad software) and stopped-flow data were analysed
205 using MATLAB. All statistical analyses were performed using Student's t-test, paired
206 Students t-test, chi-squared test, or two-way repeated measures ANOVA with Sidak
207 post hoc test, depending on the data set, as indicated in the text. $P < 0.05$ was
208 considered significant.

209

210

Results

211 Diabetics have increased glycation that correlates with myofilament function

212 We previously showed that patients with diabetes and heart failure exhibited
213 increased MG glycation of myofilament proteins, primarily actin and myosin [4]. Here,
214 we first sought to measure these MG modifications in diabetics without heart failure,
215 to test whether they might precede heart failure and represent a possible therapeutic
216 target. We utilized left ventricular (LV) tissue from donor hearts without heart failure,
217 and either with type II diabetes or without (Non-Diabetic, $n = 9$; Diabetic, $n = 6$,
218 demographic and basic clinical data shown in **Table 1**).

219

220 Table 1. Human Subject Characteristics

	Non-Diabetic	Diabetic	P-value
n	9	6	
Age (years)	63 ± 7	61 ± 10	0.82
% Female	33	50	0.62
BMI	30 ± 7	29 ± 2	0.79
% Diabetes	0	100	0.0001
% Ischemia	0	0	N/A
LVEF (%)	66 ± 7	66 ± 4	0.92
% Hypertension	22	100	0.007
Anti-hypertensive drugs (%)	16	100	0.001
Oral anti-diabetics (%)	0	66	0.01
β blockers (%)	16	50	0.23

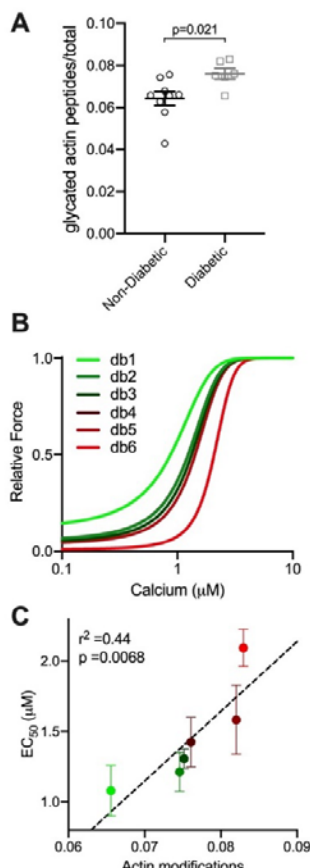
221 BMI, body mass index; LVEF, left ventricular ejection fraction. Statistics by Student's
222 t-test or Chi-squared test.

223

224 For each of these LV samples, the myofilament was enriched, separated by
225 gel electrophoresis, and the actin and myosin bands excised and analysed for MG
226 glycation by mass spectrometry. Diabetic patients exhibited significantly elevated
227 glycation (including glyoxal and methylglyoxal-derived modifications) on sarcomeric
228 actin compared to Non-Diabetic hearts (**Figure 1A, Supplemental Table 1**).
229 However, no differences were observed in myosin glycation between the groups
230 (**Supplemental Figure 1A, Supplemental Table 2**).

231 We next measured force-calcium relationships in skinned myocytes isolated
232 from LV tissue from each Diabetic heart ($n = 3 - 4$ myocytes per heart) to
233 understand the impact of increased actin glycation on sarcomere function. For each
234 Diabetic heart, the average fitted curve for all myocytes measured from that heart

235 are shown in **Figure 1B**, from the heart exhibiting the lowest level of actin glycation
236 (db1, green line) to the highest level (db6, red line). A progressive rightward shift in
237 the force-calcium relationship (calcium desensitization) was observed with increasing
238 levels of actin glycation. This correlation was confirmed when mean calcium
239 sensitivity of all cardiomyocytes from each subject was plotted against the level of
240 actin glycation for each subject (**Figure 1C**). The strong positive correlation ($r^2 =$
241 0.44, $p = 0.0068$ for a non-zero slope by linear regression), indicates that in diabetic
242 hearts, increased levels of actin glycation are associated with a progressive
243 decrease in myofilament calcium sensitivity (increased EC_{50}).



244
245 **Figure 1: Glycation of sarcomeric actin was increased in Diabetic**
246 **compared to Non-Diabetic subjects and correlates with decreased myofilament**
247 **calcium sensitivity. (A)** Glycated peptides normalized to total peptides as
248 measured by mass spectrometry on actin, from Non-Diabetic (black circles, $n=9$) and
249 Diabetic (grey squares, $n=6$) left ventricular tissue. Statistical comparison by
250 Student's t-test. **(B)** Mean fitted curves for force as a function of calcium
251 concentration in human skinned myocytes isolated from Diabetic subjects ($n=3-4$
252 myocytes per subject, $n=6$ subjects) for the subject with the lowest (db1, green) to
253 highest level of actin glycation (db6, red), showing progressive desensitization to
254 calcium in subjects with increased glycation. **(C)** Mean EC_{50} as a function of total
255 actin glycation detected by mass spectrometry for each human Diabetic sample

256 (circles colour coded from the lowest glycation level, bright green to highest glycation
257 level, bright red, $n=6$). The data are described by a positive correlation (dashed line,
258 $r^2=0.44$, $p=0.0068$ by linear regression.
259

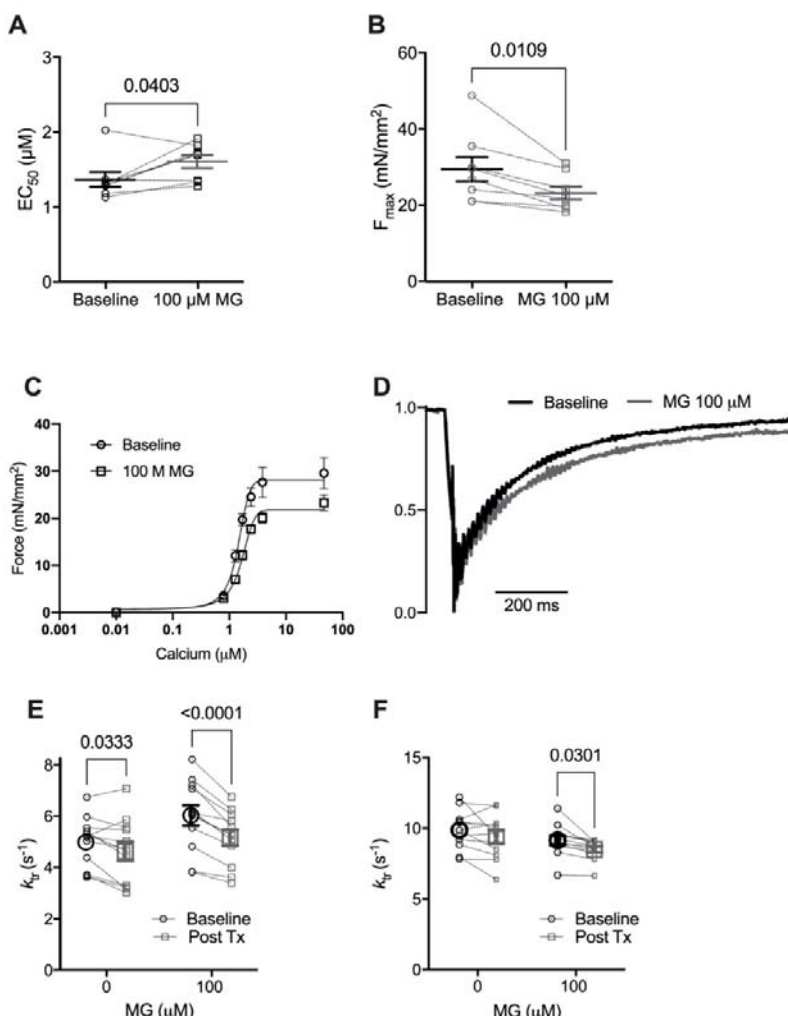
260 Not all diabetic patients eventually develop heart failure, however. Indeed,
261 while we observed increased actin glycation overall, some subjects had levels equal
262 to Non-Diabetics. As such, some subjects exhibited normal myofilament function, so
263 that no overall differences were observed in maximal calcium-activated force (F_{max})
264 or calcium sensitivity (EC_{50}) between Non-Diabetic versus Diabetic samples
265 (**Supplemental Figure 1B-D**). Myofilament calcium desensitization does not always
266 result in concurrent observable global dysfunction [23], but is known to be
267 pathogenic for dilated cardiomyopathy and heart failure. Thus, in diabetics with
268 increased glycation, MG modifications represent a possible therapeutic target to
269 reduce the risk of developing heart failure in the progression of diabetic
270 cardiomyopathy.

271
272 Computational predictions of molecular processes dysregulated by MG
273 Our next goal was to determine the molecular mechanism(s) of action of MG,
274 as myofilament functional parameters like calcium sensitivity are an aggregate
275 measurement of numerous molecular processes [24]. To predict which of these
276 processes are modified by MG we used a multiscale computer model of cooperative
277 myofilament activation [25]. To adequately constrain the model, it is necessary to
278 know the functional impact of MG on both steady-state and kinetic parameters.

279 To measure these parameters, we used skinned myocytes isolated from LV
280 tissue from three-month-old male C57Bl6/j mice treated with 100 μ M MG for 20
281 mins. In healthy tissue, levels of free MG are around 1 – 10 μ M [6, 26, 27] and
282 approximately double in disease [28]. However, the majority of MG is found on
283 glycated proteins [29], meaning these measurements of free MG significantly under-
284 estimate the amount of MG glycation that occurs. To ensure this MG treatment
285 increased glycation of the myofilament, we treated mouse left ventricular skinned
286 myocytes with 100 μ M MG for 20 mins. We then solubilized these samples, ran them
287 on SDS PAGE gels, excised actin and myosin bands, and analysed them via high
288 resolution nHPLC-MS/MS. We found that MG modifications on actin and myosin

289 were increased after the *in vitro* MG treatment (**Supplemental Figure 2 and**
290 **Supplementary Table 3, 4).**

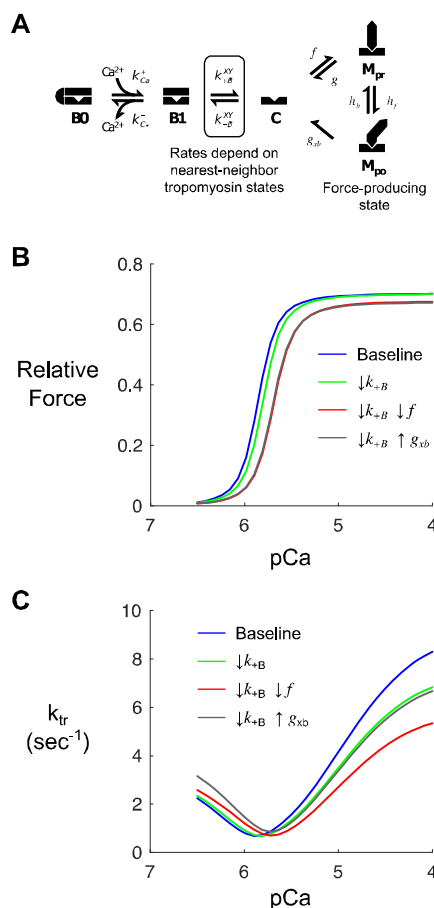
291 The impact of MG on steady-state parameters is described by the force-
292 calcium relationship. As we had shown previously [4], exposure to MG decreased
293 both calcium sensitivity and F_{\max} (**Figure 2A-C**). To determine the effect on kinetics,
294 we measured the rate of force recovery after a slack-restretch maneuver (k_{tr}) before
295 and after MG treatment. Further, k_{tr} was measured when the myocyte was exposed
296 to either maximal (46.8 μ M) or submaximal (1.7058 μ M, approximately EC₅₀)
297 calcium. Treatment with 100 μ M MG decreased k_{tr} at maximal and sub-maximum
298 Ca^{2+} activation (**Figure 2D-F**).



299
300 **Figure 2: Methylglyoxal decreases calcium sensitivity, maximal calcium-**
301 **activated force and rate of force redevelopment (k_{tr}).** (A) Individual and mean \pm
302 SEM calculated EC₅₀ (panel A) and F_{max} (panel B). (C) Mean force as a function of
303 calcium concentration and fitted curves for mouse skinned myocytes before (circles,
304 solid line) and after (squares, dashed line) exposure to 100 μ M Methylglyoxal (MG).

305 (D) Normalized k_{tr} curve before (black) and after (grey) treatment with 100 μM MG at
306 submaximal Ca^{2+} concentration (average from 12 cells). (E) Individual and mean \pm
307 SEM calculated k_{tr} values before (Baseline, black circles) or after (Post Tx, grey
308 squares) treatment with 0 (no treatment) or 100 μM MG at sub-maximal Ca^{2+}
309 concentration ($n=12$ myocytes from 4 mice, $p_{\text{interaction}} = 0.016$) (Mean \pm SEM). (F) k_{tr}
310 before (black circles) or after (grey squares) treatment with 0 or 100 μM MG at
311 maximal Ca^{2+} concentration ($n=12$ myocytes from 4 mice, $p_{\text{interaction}} = \text{n.s.}$). Statistical
312 comparisons made with 2-way repeated measures ANOVA with Sidak post-hoc test.
313

314 Next, using the computational model of myofilament activation, individual model
315 parameters were adjusted in an attempt to recapitulate the differences between the
316 baseline and MG-treated functional data (Figure 3A). The model was first used to
317 generate baseline force-calcium (blue line, Figure 3B) and k_{tr} -calcium (blue line,
318 Figure 3C) relationships, using previously published baseline model parameters
319 [25]. We then altered individual or combinations of parameters to recapitulate the
320 simultaneous impact on EC_{50} (Figure 2A), F_{max} (Figure 2B) and k_{tr} (Figure 2D-F).



321
322 **Figure 3: Computer modelling to identify potential methylglyoxal**
323 **molecular effects.** (A) Kinetic scheme for a previously published model of
324 myofilament Ca^{2+} activation [24]. The model depicts states of thin filament regulatory

325 units (B0, blocked and Ca^{2+} -free; B1, blocked and Ca^{2+} -bound; C, closed) and
326 cycling of associated myosin crossbridges (M_{pr} , myosin pre-powerstroke; M_{po} ,
327 myosin post-powerstroke). **(B)** Steady-state force-pCa curves produced by the
328 model under baseline (control) conditions and various perturbations intended to
329 qualitatively mimic observed effects of MG. Simulations show the anticipated effects
330 of slowing the blocked-closed transition of tropomyosin (k_{+B}) on its own (green) or in
331 combination with slowing myosin attachment (f , red) or myosin detachment (g , gray).
332 **(C)** Model-predicted K_{tr} -pCa relationships corresponding to the same conditions as in
333 panel B.

334

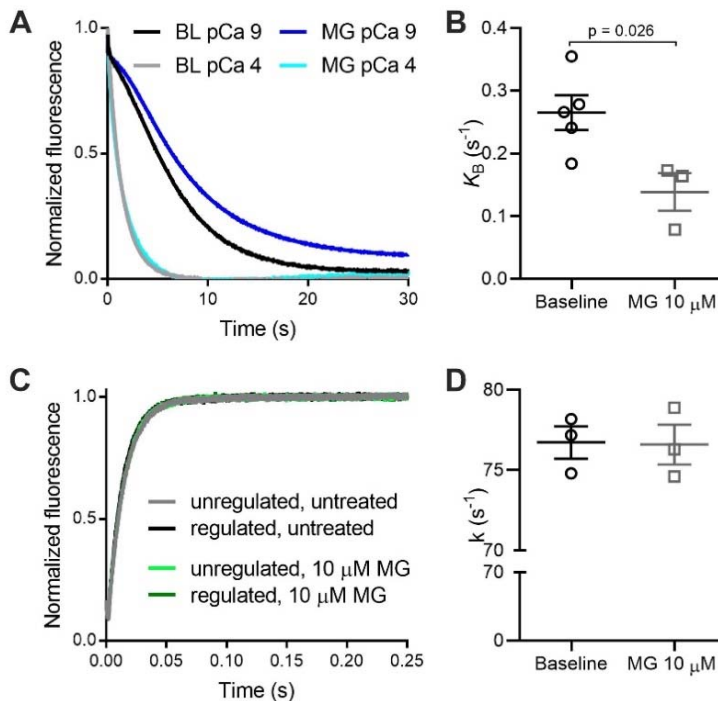
335 The model indicated that simultaneous changes in two parameters were
336 sufficient to reproduce this behaviour: 1) a ~10% decrease in the tropomyosin
337 blocked-to-closed rate transition (K_B) and 2) a decrease in the myosin crossbridge
338 duty cycle from either a 20% decrease in the myosin binding rate (f) or a 30%
339 increase in the myosin detachment rate (g_{xb}). The individual and combined effects of
340 these changes are shown in green, red, and grey on **Figure 3 B, C**. We
341 subsequently searched for experimental evidence that MG treatment affected these
342 molecular processes.

343

344 MG increases the probability of thin filaments being in the “blocked” state

345 Tropomyosin is found in three positions on actin: blocked, closed and open.
346 These positions are determined by calcium and myosin binding to the thin filament
347 [30-32]. The equilibrium constant describing the transition from the blocked to closed
348 tropomyosin state (K_B) was determined using stop flow experiments, where the rate
349 of myosin binding to pyrene-labelled regulated thin filaments was measured at high
350 (pCa 4) and low (pCa 9) calcium concentrations [22, 32]. The observed rates for
351 myosin S1 binding to the thin filament at high and low calcium were used to calculate
352 the equilibrium constant, K_B (see Supporting Materials for details). Since these
353 experiments have not been previously performed, we needed to examine the effects
354 on both the lower and the higher dose of MG on thin filaments. Stopped-flow
355 experiments were performed using reconstituted regulated thin filaments before and
356 after exposure to 10 μM MG for 20 mins. MG decreased K_B by approximately 50% in
357 regulated thin filaments (**Figure 4A, B**). A decreased equilibrium constant means
358 that the blocked state will be more favoured over the closed state. Although we
359 cannot exclude the possibility that MG decreases K_B by increasing the rate of the

360 closed-to-blocked transition, the decrease in K_B is consistent with the reduced rate of
361 the blocked-to-closed transition predicted by the computational modelling.

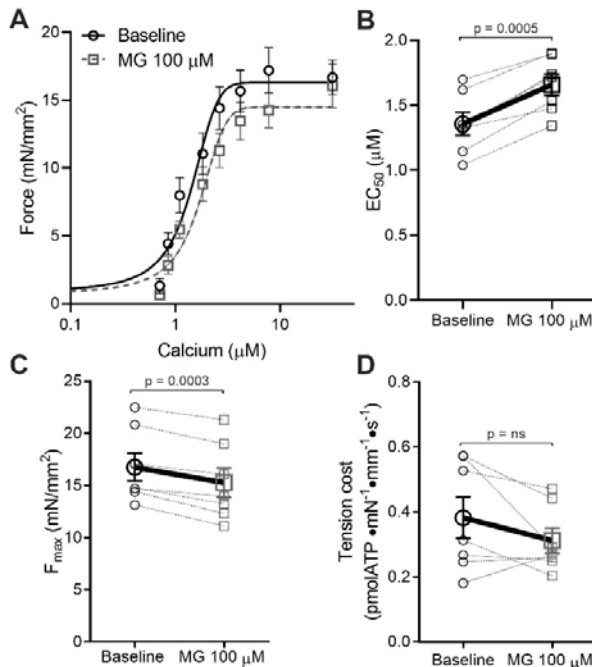


362
363 **Figure 4: Methylglyoxal decreases the tropomyosin blocked-to-closed rate**
364 **transition. (A)** Normalized fluorescence of pyrene-labelled actin as myosin S1 binds
365 to regulated thin filaments at pCa 4 (high calcium) and pCa 9 (low calcium). The
366 pyrene fluorescence decreases upon S1 binding. Rate of myosin S1 binding to
367 regulated thin filaments is higher at pCa 4 due to thin filament activation by calcium.
368 The difference in the rates at pCa 4 and pCa 9 is used to calculate K_B . The black and
369 grey lines represent untreated filaments (BL) and the dark/light blue lines represent
370 thin filaments treated with 10 μ M MG. **(B)** Individual and mean \pm SEM K_B values for
371 untreated (baseline, black dots, n=5) or treated thin filaments with 10 μ M MG (grey
372 squares, n=3). **(C)** Measurement of the actomyosin detachment rate. Normalized
373 fluorescence of pyrene-labelled actin as myosin S1 bound to ADP detaches from
374 regulated thin filaments upon addition of ATP. The rate of actomyosin detachment is
375 measured from the increase in pyrene fluorescence. Unregulated filaments (black,
376 grey) or regulated filaments (dark/light green) treated or not with 10 μ M MG. **(D)**
377 Individual and mean \pm SEM rate constant (k) for ADP release from myosin S1
378 binding to regulated thin filaments untreated (baseline, black circles) or treated with
379 10 μ M MG (grey squares) (n=3 for each). Statistical comparisons by Students t-test.
380

381 The model also predicted MG either increases the crossbridge detachment
382 rate or decreases the attachment rate. By stopped-flow, we can measure the
383 detachment rate constant (k) of ADP release from actomyosin solution, which is the
384 transition that limits crossbridge detachment rate at physiological ATP

385 concentrations. We performed stopped-flow experiments by rapidly mixing 1)
386 pyrene-labelled thin filaments pre-incubated with myosin S1 and ADP with 2)
387 solution containing saturating ATP [33]. When thin filaments were incubated with 10
388 μ M MG for 20 mins there was no difference in ADP release (**Figure 4C, D**). Even at
389 the higher 100 μ M dose, MG had no effect on the crossbridge detachment rate
390 measured using reconstituted proteins in solution (**Supplemental Figure 3**).

391 To confirm the biochemical stopped-flow results in a more physiological
392 system, we measured ATPase activity and active force production simultaneously in
393 skinned mouse papillary fibers. Tension cost (the ratio of myosin ATPase activity to
394 force production) is directly proportional to the number of post-power stroke
395 crossbridges and therefore represents a measurement of the crossbridge
396 detachment rate. We found that 40 mins incubation with MG decreased calcium
397 sensitivity and F_{max} , (as in skinned myocytes) as well as ATPase activity (**Figure 5**).
398 The longer incubation time (40 minutes vs 20 minutes in skinned cells) was
399 necessary because of the larger size of the fiber bundles. Since MG decreased both
400 force and ATPase activity in parallel, there was no effect on tension cost (the
401 ATPase activity to Force ratio), indicating that MG has no effect on the crossbridge
402 detachment rate. By two measurements we confirm that MG has no effect on the
403 crossbridge detachment rate, suggesting MG decreases the crossbridge attachment
404 rate.



405
406 **Figure 5: Methylglyoxal does not alter tension cost of mouse skinned fibers.**
407 (A) Average force-calcium data and fitted curves for skinned fibers before (black
408 circles, solid line) or after (grey squares, dashed line) treatment with 100 μM MG for
409 40 mins ($n=7$ fibers from 4 mice). (B) Individual and mean \pm SEM calculated EC₅₀
410 values before (baseline, black circles) or after 100 μM MG (grey squares). (C) F_{max}
411 before (baseline, black circles) or after 100 μM MG (grey squares) ($n=7$ fibers from 4
412 different mice). (D) Tension cost was calculated via the ratio of ATPase activity over
413 force, before (baseline, black circles) or after 100 μM MG (grey squares). Statistical
414 comparisons made by student's paired t-test.
415

416 N-terminal MyBPC fragment rescues MG-induced dysfunction but OM does not.

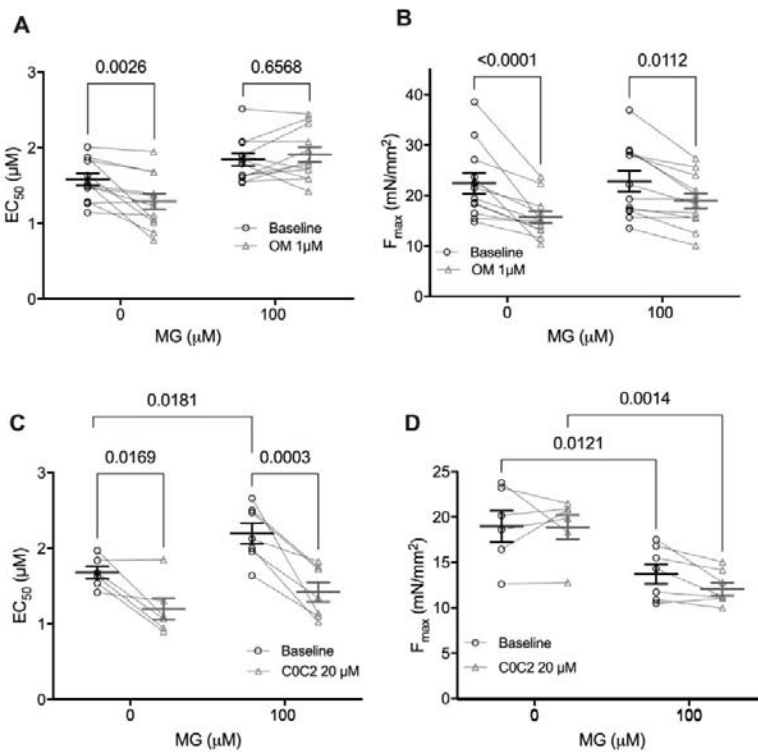
417 Having established that MG depresses myofilament function by inhibiting
418 tropomyosin movement on actin, we next aimed to determine whether we could
419 rescue calcium sensitivity by specifically targeting these mechanisms. However, we
420 first wanted to confirm that reducing MG itself is not an effective therapy. We used
421 aminoguanidine (AG), an agent that has been reported to scavenge MG and prevent
422 it from forming further modifications [34]. Skinned myocytes were pre-treated with
423 100 μM MG for 20 mins, a force-calcium relationship was measured, then treated
424 with 1 mM AG for 5 mins and a second force-calcium relationship measured. This
425 dose of AG and treatment time was chosen because previous experiments in intact
426 isolated cardiomyocytes showed it was capable of improving function [35]. However,
427 we found that AG had no effect on calcium sensitivity or F_{max} (**Supplemental Figure**
428 **4**), indicating it was unable to reverse the deleterious functional effects of MG.

429 Next, we supposed that calcium sensitizers that did not target tropomyosin
430 might be ineffective at rescuing MG-induced dysfunction. Thus, we first used
431 Omecamtiv Mecarbil (OM), a myosin activator which increases Ca^{2+} sensitivity in
432 isolated cardiomyocytes [36]. We hypothesized that MG's impact on tropomyosin
433 would block the OM-activated myosin heads from binding actin, and thus not be
434 rescued with this treatment. We found that in the absence of MG, treatment with 1
435 μM OM for 2 mins increased calcium sensitivity and decreased F_{\max} as previously
436 [36]. However, in skinned myocytes pre-incubated with 100 μM MG for 20 mins, OM
437 had no effect on Ca^{2+} sensitivity and further reduced F_{\max} (**Figure 6A,B**). These
438 results indicate that OM is not effective in reversing the functional defects by MG,
439 possibly even exacerbating the dysfunction by further reducing F_{\max} , supporting
440 MG's action through tropomyosin.

441 Knowing that MG increases the population of thin filaments in the inhibitory
442 blocked state, we next aimed to discover whether a molecule that activates the thin
443 filament could reverse the action of MG on the sarcomere. Currently, there are no
444 small molecules that act on tropomyosin [37-39], so we used recombinant cMyBPC
445 C0C2 peptide, which has been shown to activate the thin filament by pushing
446 tropomyosin into positions that are more permissive for myosin binding to the thin
447 filament [40]. The cMyBPC C0C2 peptide consists of the 466 n-terminal amino acids
448 that encompass the cardiac specific C0 domain, two Ig domains (C1, C2), a proline-
449 alanine linker between C1 and C2, and a unique cMyBPC "motif" or M-domain that
450 connects C1 and C2. We hypothesized that C0C2 would be able to reverse the
451 functional defects of MG through likewise displacing tropomyosin.

452 In mouse skinned myocytes not exposed to MG, incubation with 20 μM C0C2
453 for 20 minutes increased calcium sensitivity with no change in F_{\max} (**Figure 6C, D**),
454 which is in line with published data [41, 42]. At this concentration of C0C2, it is
455 known to interact with actin [42, 43] and is thus likely to impact tropomyosin's
456 position on actin as intended. Skinned myocytes pre-incubated with 100 μM MG
457 were significantly desensitized to calcium ($p = 0.036$ by two-way ANOVA) and
458 trended towards a decrease in F_{\max} ($p = 0.052$ by two-way ANOVA), recapitulating
459 our prior data. When these MG-preincubated myocytes were treated with C0C2 for
460 20 minutes, Ca^{2+} sensitivity was restored (from $\text{EC}_{50} = 2.19$ to 1.42, $p=0.0018$ by two-
461 way ANOVA, $n = 7$, **Figure 6C**). While there was a significant decrease in F_{\max} with

462 C0C2 treatment in the MG-exposed myocytes (from $F_{max} = 13.9$ to 12.2, $p=0.043$ by
463 two-way ANOVA, $n = 7$, **Figure 6D**), the magnitude of this decrease was less than
464 15% of the pre-treatment level and is likely due to normal myocyte rundown during
465 multiple activations. Furthermore, there was no interaction between C0C2 and MG
466 treatments on the effect of F_{max} ($p = 0.57$ by two-way ANOVA). Overall, these data
467 show that C0C2 can reverse the depressed calcium sensitivity caused by MG,
468 presumably by moving tropomyosin on actin into a position that is favourable for
469 myosin contraction.



470
471 **Figure 6: C0C2 rescues the calcium sensitivity decrease caused by MG in**
472 **skinned cardiomyocytes but OM does not.** (A) Individual and mean ± SEM EC₅₀
473 values from skinned myocytes pre-exposed to 0 μM MG ($n=6$) or 100 μM MG ($n=7$
474 from 3-4 mice) before treatment with cardiac myosin binding protein C peptide C0C2
475 (baseline, black circles) or after (C0C2 20 μM, grey triangles). Paired before and
476 after data for an individual cell are connected by dashed lines. (B) Individual and
477 mean ± SEM F_{max} values from skinned myocytes pre-exposed with 0 μM MG ($n=4$)
478 or 100 μM MG ($n=7$ from 3 mice) before with C0C2 (baseline, black circles) or after
479 (C0C2 20 μM, grey triangles). Individual and mean ± SEM calculated EC₅₀ (panel G)
480 and F_{max} (panel F) from skinned myocytes pre-exposed to 0 μM MG ($n=8$) or 100 μM
481 MG ($n=12$ from 4 mice) before (baseline, black circles) or after treatment with 1 μM
482 Omecamtiv Mecarbil (1 μM OM, grey triangles) ($n=12$ myocytes from 4 mice). Paired
483 before and after treatment data for each individual cell are connected by dashed
484 lines. Statistical comparisons by two-way repeated measures ANOVA with Sidak
485 post-hoc test.

486

Discussion

487 We have shown for the first time that diabetics free of heart failure exhibit
488 increased MG actin glycation compared to those without diabetes. In diabetics, the
489 magnitude of elevated glycation positively correlated with myofilament
490 desensitization to calcium. Not all diabetics eventually develop heart failure, so it is
491 reasonable that in this cohort we would detect a range of glycation and function. It is
492 thus unlikely that overt dysfunction could be used to predict the eventual
493 development of heart failure in diabetics, and MG modifications may represent a
494 more sensitive biomarker. We hypothesize those subjects with high levels of
495 glycation and calcium desensitization would be the most likely to develop diabetic
496 cardiomyopathy and heart failure [2]. As these were donor hearts, it is impossible to
497 know for sure whether they would have eventually developed cardiac dysfunction,
498 however, point mutations that cause familial dilated cardiomyopathy frequently cause
499 similar myofilament calcium desensitization that eventually leads to heart failure [12].
500 Thus, the cellular dysfunction induced by this glycation represents a possible
501 therapeutic target for inhibiting the development of diabetic cardiomyopathy [44],
502 which can lead to heart failure [45].

503 In non-failing diabetics, the median magnitude of the increase in actin
504 glycation was about half of what we previously observed in diabetic patients with
505 heart failure (~20% vs ~40% increase compared to controls [4]). This relationship
506 suggests that myofilament MG glycation increases in parallel with disease severity,
507 preceding global cardiac dysfunction. Importantly, while our previous work was in
508 diabetic heart failure patients [4], these findings in otherwise healthy diabetics
509 decouple the impact of myofilament glycation on cardiomyocyte function from
510 adaptive and maladapting processes occurring during end-stage heart failure. That
511 the increased glycation was detected only on actin, and not myosin, was unexpected
512 but suggests a preference for MG glycation. While no previous studies have
513 identified any site specificity for MG glycation, these data indicate there are certainly
514 preferred targets, possibly due to length or concentration of MG exposure as well as
515 the accessibility and reactivity of the modified residues. The increased levels of MG
516 glycation on solely actin are still harmful as our previous work showed dysfunction
517 was induced by MG glycation of actin or myosin independently [4].

518 Unfortunately, broadly targeting the MG-induced dysfunction with compounds
519 that inhibit MG modifications or general systolic activators was unsuccessful in

520 reversing the dysfunction. A combination of biophysical functional approaches,
521 computer simulation, and stopped-flow experiments revealed that MG modifications
522 increase the population of the tropomyosin blocked state, therefore inhibiting myosin
523 from binding to the thin filament and initiating contraction. Effectively, MG makes it
524 more difficult to activate the thin filaments to allow force production. By targeting this
525 mechanism specifically, using a thin-filament interacting peptide of myosin binding
526 protein C, we were thus able to rescue MG-induced calcium desensitization.

527 Our previously published mass spectrometry data provides a possible
528 mechanism for how MG affects tropomyosin movement. We found MG glycation of
529 actin K291 [4], which is within a critical region of actin termed the “A-triad”, a cluster
530 which stabilizes the A-state structure, which is similar to the blocked state [46].
531 Mutations and modifications to residues in this region have been shown to alter
532 function by either stabilizing or de-stabilizing the A-state [47]. We propose that MG
533 forms an irreversible glycation modification on K291 residue in the A-triad, changing
534 the allosteric interactions between actin and tropomyosin to stabilize the blocked
535 state of tropomyosin and therefore reduce K_B and myofilament calcium sensitivity
(Supplemental Figure 5).

537 The computer model also predicted MG glycation inhibits the crossbridge duty
538 cycle, although the model is unable to differentiate between either a decrease in f
539 (crossbridge attachment rate) or an increase in g (crossbridge detachment rate). The
540 stopped flow and tension cost data both indicated that the detachment rate was
541 unchanged. Combined with the model, these data highly suggest that MG decreases
542 the crossbridge attachment rate. Unfortunately, measuring the attachment rate
543 requires proteins in saturated conditions (i.e., non-physiological), and is challenging
544 to measure with rigorous approaches, so this cannot be confirmed at present.
545 However, one possible explanation for how MG could decrease the attachment rate
546 is by affecting the super-relaxed state of myosin [48]. If MG enhances the super-
547 relaxed state and fewer myosin heads are available to form crossbridges, this could
548 appear as a reduced rate of attachment (f). The stopped-flow experiments do not
549 include the impact of the super-relaxed state, so it is not possible to account for its
550 effect. Furthermore, while the tension cost experiments presumably do include the
551 super-relaxed state, myosin heads in this state have a very low basal ATPase
552 activity [49] and might have little effect on the measured tension cost. Thus, whether

553 MG alters the super-relaxed state remains an unaccounted-for possibility in this
554 study.

555 Our results in myocytes not exposed to MG agree with prior studies showing
556 OM increases myofilament calcium sensitivity [36] and reduces F_{max} likely by
557 depressing the myosin working stroke [50]. We showed that MG blocked the calcium
558 sensitizing effect of OM but did not affect its ability to decrease F_{max} , indicating that
559 MG causes OM to act as a negative inotrope. Our finding that MG keeps
560 tropomyosin in the “blocked” position can mechanistically explain this effect. First,
561 OM primes myosin heads to increase their binding to actin to form force-generating
562 crossbridges at submaximal calcium [51], but since MG inhibits thin filament
563 activation, this calcium sensitizing effect is blocked. Furthermore, OM decreases
564 F_{max} by decreasing the myosin working stroke, which would be unaffected by
565 tropomyosin positioning.

566 Finally, the C0C2 domains of cMyBPC were able to restore the MG-induced
567 decrease in calcium sensitivity. The mechanism of C0C2’s benefit is likely by
568 counteracting the MG-induced reduction in tropomyosin’s blocked-to-closed
569 transition rate, as it has been suggested that C0C2 can alter tropomyosin’s position
570 on actin [18, 52]. These findings provide a strong proof-of-principle that specifically
571 targeting the molecular mechanism of MG can rescue function. However, the C0C2
572 peptide was not able to restore the decrease in F_{max} caused by MG. The inability of
573 C0C2 to restore F_{max} supports the model prediction that there are two separate
574 effects of MG glycation on the sarcomere, and C0C2 only affects one of these.
575 Whether this second effect is a decrease in the crossbridge attachment rate as the
576 model and experiments suggest and if this dysfunction can likewise be reversed will
577 have to be determined in future studies. Furthermore, whether the C0C2 cMyBPC
578 fragment could be an appropriate therapeutic option in the clinic is not clear. The
579 C0C2 peptide contains the regulatory region of cMyBPC that includes
580 phosphorylation sites that are important for the sarcomere’s response adrenergic
581 stimulation [43, 53, 54], so the peptide would be susceptible to modulation by
582 phosphorylation *in vivo*. However, a recent study expressed the C0C2 peptide using
583 AAV, and showed it was capable of rescuing function in a cMyBPC knockout mouse
584 [55], suggesting the peptide is stable and functional *in vivo*.

585

586 **Conclusion**

587 Overall, this study provides a proof of principal that either C0C2 or another
588 therapeutic that can move tropomyosin towards the “open” state would be a potential
589 therapeutic avenue for patients who have diabetes and either have heart failure or
590 are at risk of developing it. As initial treatment approaches failed, such as AGE-
591 breakers, it was critical that we identified this specific mechanism of MG glycation
592 using biophysical, computational, and chemical kinetics. Furthermore, as no small
593 molecules currently target tropomyosin, these results provide rationale that future
594 drug discovery efforts should explore this mechanism. These insights provide a
595 strong foundation for future work targeting these mechanisms to stem the increase in
596 heart failure cases that will occur as the prevalence of diabetes continues to grow
597 worldwide.

598

599 **Funding:** This work was funded by the American Heart Association
600 (111POST7210031 to M.P.), the National Institutes of Health (R01HL136737 to
601 J.A.K. and R01HL 141086 to M.J.G), the Children’s Discovery Institute of
602 Washington University and St. Louis Children’s Hospital (PM-LI-2019-829 to M.J.G.),
603 the Austrian Science Fund (I 4168-B to P.P.R.), and the European Research Area
604 Network (ERA-CVD to P.P.R.).

605

606 **Author contribution:** M.P. and J.A.K. designed the project and research studies.
607 M.P., T.K., S.K.B. and S.G.C. conducted experiments and acquired data. M.P.,
608 S.K.B., S.C.G., M.J.G. and J.A.K. interpreted experimental results. M.P., S.G.C. and
609 J.A.K. analysed data and created figures. P.P.R., D.L. and S.P.H. provided peptide
610 and human samples. M.P. and J.A.K. wrote the manuscript. T.K., S.K.B., S.G.C.,
611 D.L., P.P.R., S.P.H. and M.J.G. revised the manuscript.

612

613 **Conflict of Interest:** None declared

614

615

References

- 616 1. Saeedi, P., et al., *Global and regional diabetes prevalence estimates for 2019*
617 *and projections for 2030 and 2045: Results from the International Diabetes*
618 *Federation Diabetes Atlas, 9(th) edition.* Diabetes Res Clin Pract, 2019. **157**:
619 p. 107843.
- 620 2. Kenny, H.C. and E.D. Abel, *Heart Failure in Type 2 Diabetes Mellitus.* Circ
621 Res, 2019. **124**(1): p. 121-141.
- 622 3. Dei Cas, A., et al., *Impact of diabetes on epidemiology, treatment, and*
623 *outcomes of patients with heart failure.* JACC Heart Fail, 2015. **3**(2): p. 136-
624 45.
- 625 4. Papadaki, M., et al., *Diabetes with heart failure increases methylglyoxal*
626 *modifications in the sarcomere, which inhibit function.* JCI Insight, 2018. **3**(20).
- 627 5. Phillips, S.A. and P.J. Thornalley, *The formation of methylglyoxal from triose*
628 *phosphates. Investigation using a specific assay for methylglyoxal.* Eur J
629 Biochem, 1993. **212**(1): p. 101-5.
- 630 6. Rabbani, N. and P.J. Thornalley, *Methylglyoxal, glyoxalase 1 and the*
631 *dicarbonyl proteome.* Amino Acids, 2012. **42**(4): p. 1133-42.
- 632 7. Hegab, Z., et al., *Role of advanced glycation end products in cardiovascular*
633 *disease.* World J Cardiol, 2012. **4**(4): p. 90-102.
- 634 8. Soman, S., et al., *A multicellular signal transduction network of AGE/RAGE*
635 *signaling.* J Cell Commun Signal, 2013. **7**(1): p. 19-23.
- 636 9. Schalkwijk, C.G. and C.D.A. Stehouwer, *Methylglyoxal, a Highly Reactive*
637 *Dicarbonyl Compound, in Diabetes, Its Vascular Complications, and Other*
638 *Age-Related Diseases.* Physiol Rev, 2020. **100**(1): p. 407-461.
- 639 10. Shao, C.H., et al., *Carbonylation contributes to SERCA2a activity loss and*
640 *diastolic dysfunction in a rat model of type 1 diabetes.* Diabetes, 2011. **60**(3):
641 p. 947-59.
- 642 11. Shao, C.H., et al., *Carbonylation induces heterogeneity in cardiac ryanodine*
643 *receptor function in diabetes mellitus.* Mol Pharmacol, 2012. **82**(3): p. 383-99.
- 644 12. Du, C.K., et al., *Knock-in mouse model of dilated cardiomyopathy caused by*
645 *troponin mutation.* Circ Res, 2007. **101**(2): p. 185-94.
- 646 13. Alomar, F.A., et al., *Adeno-Associated Viral Transfer of Glyoxalase-1 Blunts*
647 *Carbonyl and Oxidative Stresses in Hearts of Type 1 Diabetic Rats.*
648 Antioxidants (Basel), 2020. **9**(7).
- 649 14. Moreau, R., et al., *Reversal by aminoguanidine of the age-related increase in*
650 *glycoxidation and lipoxidation in the cardiovascular system of Fischer 344*
651 *rats.* Biochem Pharmacol, 2005. **69**(1): p. 29-40.
- 652 15. Dhar, A., et al., *Alagebrium attenuates methylglyoxal induced oxidative stress*
653 *and AGE formation in H9C2 cardiac myocytes.* Life Sci, 2016. **146**: p. 8-14.
- 654 16. Engelen, L., C.D. Stehouwer, and C.G. Schalkwijk, *Current therapeutic*
655 *interventions in the glycation pathway: evidence from clinical studies.*
656 Diabetes Obes Metab, 2013. **15**(8): p. 677-89.
- 657 17. Marston, S., *Small molecule studies: the fourth wave of muscle research.* J
658 Muscle Res Cell Motil, 2019. **40**(2): p. 69-76.
- 659 18. Risi, C., et al., *N-Terminal Domains of Cardiac Myosin Binding Protein C*
660 *Cooperatively Activate the Thin Filament.* Structure, 2018. **26**(12): p. 1604-
661 1611 e4.
- 662 19. Kirk, J.A., et al., *Pacemaker-induced transient asynchrony suppresses heart*
663 *failure progression.* Sci Transl Med, 2015. **7**(319): p. 319ra207.

664 20. de Tombe, P.P. and G.J. Stienen, *Impact of temperature on cross-bridge*
665 *cycling kinetics in rat myocardium*. J Physiol, 2007. **584**(Pt 2): p. 591-600.

666 21. Lin, B.L., et al., *Skeletal myosin binding protein-C isoforms regulate thin*
667 *filament activity in a Ca(2+)-dependent manner*. Sci Rep, 2018. **8**(1): p. 2604.

668 22. Barrick, S.K., et al., *Computational Tool to Study Perturbations in Muscle*
669 *Regulation and Its Application to Heart Disease*. Biophys J, 2019. **116**(12): p.
670 2246-2252.

671 23. Westfall, M.V., et al., *Myofilament calcium sensitivity and cardiac disease:*
672 *insights from troponin I isoforms and mutants*. Circ Res, 2002. **91**(6): p. 525-
673 31.

674 24. Mamidi, R., et al., *Lost in translation: Interpreting cardiac muscle mechanics*
675 *data in clinical practice*. Arch Biochem Biophys, 2019. **662**: p. 213-218.

676 25. Sheikh, F., et al., *Mouse and computational models link Mlc2v*
677 *dephosphorylation to altered myosin kinetics in early cardiac disease*. J Clin
678 Invest, 2012. **122**(4): p. 1209-21.

679 26. Phillips, S.A., D. Mirrlees, and P.J. Thronalley, *Modification of the glyoxalase*
680 *system in streptozotocin-induced diabetic rats and the effect of the aldose*
681 *reductase inhibitor Statiil*. Biochem Soc Trans, 1993. **21**(2): p. 162S.

682 27. Dobler, D., et al., *Increased dicarbonyl metabolism in endothelial cells in*
683 *hyperglycemia induces anoikis and impairs angiogenesis by RGD and*
684 *GFOGER motif modification*. Diabetes, 2006. **55**(7): p. 1961-9.

685 28. Rabbani, N. and P.J. Thronalley, *Glyoxalase in diabetes, obesity and related*
686 *disorders*. Semin Cell Dev Biol, 2011. **22**(3): p. 309-17.

687 29. Lo, T.W., et al., *Binding and modification of proteins by methylglyoxal under*
688 *physiological conditions. A kinetic and mechanistic study with N alpha-*
689 *acetylarginine, N alpha-acetylcysteine, and N alpha-acetylysine, and bovine*
690 *serum albumin*. J Biol Chem, 1994. **269**(51): p. 32299-305.

691 30. Lehman, W., R. Craig, and P. Vibert, *Ca(2+)-induced tropomyosin movement*
692 *in Limulus thin filaments revealed by three-dimensional reconstruction*.
693 Nature, 1994. **368**(6466): p. 65-7.

694 31. Vibert, P., R. Craig, and W. Lehman, *Steric-model for activation of muscle thin*
695 *filaments*. J Mol Biol, 1997. **266**(1): p. 8-14.

696 32. McKillop, D.F. and M.A. Geeves, *Regulation of the interaction between actin*
697 *and myosin subfragment 1: evidence for three states of the thin filament*.
698 Biophys J, 1993. **65**(2): p. 693-701.

699 33. Clippinger, S.R., et al., *Disrupted mechanobiology links the molecular and*
700 *cellular phenotypes in familial dilated cardiomyopathy*. Proc Natl Acad Sci U S
701 A, 2019. **116**(36): p. 17831-17840.

702 34. Lo, T.W., T. Selwood, and P.J. Thronalley, *The reaction of methylglyoxal with*
703 *aminoguanidine under physiological conditions and prevention of*
704 *methylglyoxal binding to plasma proteins*. Biochem Pharmacol, 1994. **48**(10):
705 p. 1865-70.

706 35. Ziolo, M.T., S.J. Dollinger, and G.M. Wahler, *Myocytes isolated from rejecting*
707 *transplanted rat hearts exhibit reduced basal shortening which is reversible by*
708 *aminoguanidine*. J Mol Cell Cardiol, 1998. **30**(5): p. 1009-17.

709 36. Nagy, L., et al., *The novel cardiac myosin activator omecamtiv mecarbil*
710 *increases the calcium sensitivity of force production in isolated*
711 *cardiomyocytes and skeletal muscle fibres of the rat*. Br J Pharmacol, 2015.
712 **172**(18): p. 4506-4518.

713 37. Psotka, M.A., et al., *Cardiac Calcitropes, Myotropes, and Mitotropes: JACC Review Topic of the Week*. *J Am Coll Cardiol*, 2019. **73**(18): p. 2345-2353.

714 38. Pollesello, P., Z. Papp, and J.G. Papp, *Calcium sensitizers: What have we learned over the last 25 years?* *Int J Cardiol*, 2016. **203**: p. 543-8.

715 39. Alsulami, K. and S. Marston, *Small Molecules acting on Myofilaments as Treatments for Heart and Skeletal Muscle Diseases*. *Int J Mol Sci*, 2020. **21**(24).

716 40. Mun, J.Y., et al., *Myosin-binding protein C displaces tropomyosin to activate cardiac thin filaments and governs their speed by an independent mechanism*. *Proc Natl Acad Sci U S A*, 2014. **111**(6): p. 2170-5.

717 41. Herron, T.J., et al., *Activation of myocardial contraction by the N-terminal domains of myosin binding protein-C*. *Circ Res*, 2006. **98**(10): p. 1290-8.

718 42. Razumova, M.V., et al., *Contribution of the myosin binding protein C motif to functional effects in permeabilized rat trabeculae*. *J Gen Physiol*, 2008. **132**(5): p. 575-85.

719 43. Shaffer, J.F., R.W. Kensler, and S.P. Harris, *The myosin-binding protein C motif binds to F-actin in a phosphorylation-sensitive manner*. *J Biol Chem*, 2009. **284**(18): p. 12318-27.

720 44. Boudina, S. and E.D. Abel, *Diabetic cardiomyopathy, causes and effects*. *Rev Endocr Metab Disord*, 2010. **11**(1): p. 31-9.

721 45. Jia, G., M.A. Hill, and J.R. Sowers, *Diabetic Cardiomyopathy: An Update of Mechanisms Contributing to This Clinical Entity*. *Circ Res*, 2018. **122**(4): p. 624-638.

722 46. Viswanathan, M.C., et al., *Distortion of the Actin A-Triad Results in Contractile Disinhibition and Cardiomyopathy*. *Cell Rep*, 2017. **20**(11): p. 2612-2625.

723 47. Schmidt, W. and A. Cammarato, *The actin 'A-triad's' role in contractile regulation in health and disease*. *J Physiol*, 2019.

724 48. McNamara, J.W., et al., *The role of super-relaxed myosin in skeletal and cardiac muscle*. *Biophys Rev*, 2015. **7**(1): p. 5-14.

725 49. Stewart, M.A., et al., *Myosin ATP turnover rate is a mechanism involved in thermogenesis in resting skeletal muscle fibers*. *Proc Natl Acad Sci U S A*, 2010. **107**(1): p. 430-5.

726 50. Woody, M.S., et al., *Positive cardiac inotrope omecamtiv mecarbil activates muscle despite suppressing the myosin working stroke*. *Nat Commun*, 2018. **9**(1): p. 3838.

727 51. Planelles-Herrero, V.J., et al., *Mechanistic and structural basis for activation of cardiac myosin force production by omecamtiv mecarbil*. *Nat Commun*, 2017. **8**(1): p. 190.

728 52. Inchingolo, A.V., et al., *Revealing the mechanism of how cardiac myosin-binding protein C N-terminal fragments sensitize thin filaments for myosin binding*. *Proc Natl Acad Sci U S A*, 2019. **116**(14): p. 6828-6835.

729 53. Colson, B.A., et al., *Site-directed spectroscopy of cardiac myosin-binding protein C reveals effects of phosphorylation on protein structural dynamics*. *Proc Natl Acad Sci U S A*, 2016. **113**(12): p. 3233-8.

730 54. Gresham, K.S. and J.E. Stelzer, *The contributions of cardiac myosin binding protein C and troponin I phosphorylation to beta-adrenergic enhancement of in vivo cardiac function*. *J Physiol*, 2016. **594**(3): p. 669-86.

731 55. Li, J., et al., *AAV9 gene transfer of cMyBPC N-terminal domains ameliorates cardiomyopathy in cMyBPC-deficient mice*. *JCI Insight*, 2020. **5**(17).

732

733

734

735

736

737

738

739

740

741

742

743

744

745

746

747

748

749

750

751

752

753

754

755

756

757

758

759

760

761

762